

Wind resources and wind farm wake effects offshore observed from satellite

Charlotte Bay Hasager, Poul Astrup, Merete Bruun Christiansen, Morten Nielsen, Rebecca Barthelmie
Risø National Laboratory, Wind Energy Department, Roskilde, Denmark

Charlotte.hasager@risoe.dk, poul.astrup@risoe.dk, merete.bruun.Christiansen@risoe.dk, morten.Nielsen@risoe.dk, r.barthelmie@risoe.dk

Abstract:

Satellite observations of ocean wind speed and wind direction are obtained from different satellite sources; the data are used to estimate the wind resource of the Danish Seas. The wind maps are based on three types of satellite observing techniques: passive microwave, scatterometer and Synthetic Aperture Radar (SAR). From passive microwave a 17-year long time series is used and from scatterometer a 5-year long time series. Two data series based on SAR are analyzed. One consists of 55 maps in very high spatial resolution (400 m grid cells) covering Horns Rev in the North Sea; the other 25 maps in medium spatial resolution (1.6 km grid cells) covering Denmark. Comparison results to mast observations are presented. Very high resolution SAR wind maps are used to quantify the wake effect at two large offshore wind farms in Denmark. It is found that the wake velocity deficit is around 10% at 0 to 3 km downwind and that the wind recovers to 2% of the upstream values at around 4 to 18 km downstream as a function of atmospheric stability. The recovery is faster for unstable than for near-neutral conditions.

Keywords: satellite, offshore wind resource, wake.

1 Introduction

In Europe the wind energy potential offshore is considerably greater than onshore (1). Due to the rising cost on oil and gas 'energy without fuel' (2) may, at a political level, accelerate wind energy plans further. There is fast progress on planning and installation of offshore wind farms in the European waters including Denmark, the UK, Ireland, Sweden, Germany, the Netherlands, etc. Offshore activities are also in progress in several Asian countries and North America. This reinforces activities related to offshore development. One challenge is to assess external conditions for offshore wind farms rapidly and

accurately. The wind resource is one of the most important external conditions.

It is well known that offshore meteorological observations are sparse and costly. Therefore the offshore wind climate has not yet been mapped in great detail. Furthermore model results on offshore wind climates are not fully verified due to lack of appropriate meteorological observations. Modelling wind in the coastal zone is challenging as the atmospheric flow typically traverses a variation both in roughness and temperature at the coastline. This causes internal boundary layers to develop. At several coastal sites are observed land- and sea-breeze effects, tunneling effects through belts, sounds and fjords, and katabatic flow, e.g. in the Mediterranean Seas. These physical phenomena add to the complexity of wind modelling in coastal areas of interest for offshore wind farming.

Satellite ocean wind observations constitute a complementary source of information to meteorological mast data and model results. Advantages of satellite wind maps are:

- Some satellite wind maps are free of cost¹
- All offer global coverage
- All are accessible in archives spanning several years
- The accuracy is sufficient for pre-feasibility studies
- Satellite wind maps quantify spatial variations
- Wind resource maps are available in resolutions of 400 m, 1.6 km and 0.25°,
- Software and services have been developed for applied use.²

There are also limitations:

¹ <http://podaac.jpl.nasa.gov/products/product108.htm>

² <http://www.eo-windfarm.org/>,

<http://www.risoe.dk/vea-atu/remote/EOWindfarm.htm>

- The accuracy is around 1.2 to 1.5 ms^{-1} standard deviation on mean wind speed (not bankable)
- Satellites determine wind from surface properties which are translated into 10 m winds.

Very high-resolution wind maps from SAR can provide quantitative estimates of the wake velocity deficit downstream of large offshore wind farms. This information is of interest for areas in which wind farm clusters are in preparation.

In summary, satellite wind maps are accessible today at different grid resolutions and the observations can be used as a complementary source of information for offshore wind resource mapping. This task is of high priority in many regions of the world as offshore wind farming is in rapid growth. The paper describes the state-of-the-art on wind resource estimation based on satellite wind observations offshore. Chapter 2 contains detail on the various satellite sources used in the current study. Chapter 3 presents results. Discussion and conclusion are found in Chapter 4 and 5, respectively.

2 Satellite wind maps

Ocean winds have been collected routinely since the mid-1980s from satellites. At the onset these data were classified, hence not generally available. The observations were obtained from passive microwave providing wind speed at relatively low spatial resolution yet frequently in time. From the early 1990s this situation changed with the launch of scatterometers and SAR instruments on research platforms. Both types of instruments provide observations from which wind vectors can be determined. Since the late 1990s scatterometers operationally provide global ocean wind vector maps. Passive microwave polarimetric radiometer wind vector data are available since 2003 at research level and are foreseen to become operational in a few years. Some ocean wind data are available only in swath mode, i.e. the original coordinate system; most ocean wind maps are available in gridded mode, i.e. resampled to a geographical coordinate system.

2.1 Passive microwave

It is the Meteorological Program of the United States Department of Defense that is in charge of the Defense Meteorological Satellite Program (DMPS). Within DMPS a long series of Earth observing satellite have been active since the mid-1970s. This series is called F-1 (from 1976), F-2 (from 1977), etc. up to currently operating satellite platforms F-13

(from 1995), F-14 (from 1997), and F-15 (from 1999). Since F-8 (from 1987) a passive microwave radiometer has been flown. This sensor is capable of measuring ocean wind speed. It is the Special Sensor Microwave Imager (SSM/I).

SSM/I

SSM/I is a seven channel, four frequency, linearly-polarized, passive microwave radiometric system which measures atmospheric, ocean, and terrain microwave brightness temperatures at 19.35, 22.24, 37.00 and 85.80 GHz (3). The archived data consists of antenna temperatures recorded across a 1400 km swath. The brightness temperature (T_B) in Kelvin is related to the instantaneous wind speed over the ocean. An empirical relationship is found between T_B and wind observations from buoys and radiosondes. It is the wind speed at 10 m above sea surface that is calculated (4). Recently the SSM/I data series have been recalculated (http://www.ssmi.com/ssmi/ssmi_description.html).

The dynamic range is 3-25 ms^{-1} with a target accuracy of $\pm 2\text{ms}^{-1}$ or 1.3 ms^{-1} rms. (root mean square) in global maps with grid resolution of 0.25°. Local equator crossing times are for F-8, F-19 and F-13 at 6.00 and 18.00; for F-11 at 5.00 and 17.00; for F-14 at 9.30 and 20.30; and for F-15 at 10.30 and 21.30.

AMSR-E

The Advanced Microwave Scanning Radiometer - Earth Observing System (AMSR-E) is a twelve-channel, six-frequency, passive-microwave radiometer system. It measures horizontally and vertically polarized brightness temperatures at 6.9, 10.7, 18.7, 23.8, 36.5 and 89.0 GHz. AMSR-E was developed by Japan Aerospace Exploration Agency (JAXA). AMSR-E was launched in April 2002. The dynamic range is 0-30 ms^{-1} with a target accuracy of $\pm 2\text{ms}^{-1}$ (0-20 ms^{-1}) and 10% rms (0-30 ms^{-1}) in global maps with grid resolution of 0.25°. Local equator crossing time is at 10.30 and 21.30.

WindSat

The WindSat radiometer on-board the Coriolis satellite platform is the first space-borne multi-frequency polarimetric microwave radiometer. It was launched January 2003. WindSat was developed by the Naval Research Laboratory for the U.S. Navy and the National Polar-orbiting Operational Environmental Satellite System. It will be used instead of SSM/I after year 2010 when the DMPS and National Oceanic and Atmospheric Administration (NOAA) meteorological programs merge. Furthermore the European MetOp ASCAT (Advanced Scatterometer) will be part of this new system. MetOp

is the European EUMETSAT space segment of polar orbiters from year 2006 to 2020. WindSat has a 840 km swath and provides global ocean wind vector maps at research level.

2.2 Scatterometer

Scatterometers are real aperture radars operating in the microwave spectrum either at ~ 5 GHz (C-band) or ~ 13 GHz (Ku-band). The European (ERS AMI and ASCAT) scatterometers work at C-band whereas the American/Japanese scatterometers (SASS, NSCAT, QuikSCAT and Midori-2) work at Ku-band.

Scatterometers transmit pulses. The pulses are echoed back to the instrument and received. The transmitted pulse is a pulse with linear frequency modulation ('chirp'). When the received pulses are de-chirped, the backscattered signal can be analyzed. The frequency can be mapped into slant range when the chirp rate and the Doppler frequency are known. The normalized backscatter per resolution cell in slant range (across track) and ground range (along flight track) is the key information used for wind vector retrieval. Variations in the magnitude of the Normalized Radar Cross Section (NRCS) are a function of the centimeter-sized, wind-driven waves of the ocean surface.

QuikSCAT

QuikSCAT was launched in June 1999 by NASA and JAXA (formerly NASDA). QuikSCAT belongs to NASA/JPL (National Aeronautics and Space Administration/Jet Propulsion Lab.. The SeaWinds scatterometer on board the QuikSCAT satellite platform has two pencil beam radar antennae both scanning in conical shape. The two antennae measure with two different incident angles, two polarizations, and as the beams look forward and aft, also measure at two different aspect angles. Hence multiple NRCS observations are obtained at ~25 km resolution. The three backscatter-measurements of each grid point are obtained at different viewing angles and separated by a short time delay. These "triplets" are fed to a mathematical model that calculates surface wind speed and direction. The mathematical model is a geophysical model function (GMF) that relates the NRCS to the wind vector through empirical coefficients. The coefficients are found from collocated in-situ wind data and NRCS values, or a combination of in-situ wind data, meteorological model data and NRCS values (5). Nominal accuracies are $\pm 2 \text{ ms}^{-1}$ or 10% rms. on wind speed and $\pm 20^\circ$ on direction for the range of 3 to 20 ms^{-1} .

2.3 Synthetic Aperture Radar (SAR)

A SAR instrument is looking sideways between the angles from near-range to far-range. In this dimension, the slant range observations are made. The distance on the ground between near- and far-range is the swath width. The across track resolution is obtained through frequency modulation ('chirp'). As the satellite moves along the flight track, the azimuth range observations are made. The azimuth resolution is specified as one-half the antenna length. The synthetic aperture is obtained by tracking the individual phase and amplitude of individual return signals during a given integration time interval. Hence the distance is much longer than the physical length of the instrument antenna. It is the Doppler shift in each individual recorded signal in the backscatter signal that determines the position of the scatter in the azimuth position.

The SAR illuminates a footprint and the signals returned from the footprint area are the backscattered values, the NRCS. It is again the relationship between NRCS and ocean wind speed, similar to scatterometers, which is used to calculate the wind speed. The geophysical model functions can be used provided that the wind direction is known *a priori*, as the imaging SAR obtains only one view of the surface (in contrast to e.g. 3 to 4 views from the antennae at scatterometers). In most SAR images it is possible to identify linear features aligned with the mean wind direction from techniques such as two-dimensional Fast Fourier analysis (6, 7), wavelets (8) or local gradient (9, 10).

In contrast to scatterometers that are designed to map ocean winds operationally, SAR systems serve a multitude of (research) tasks. Therefore a systematic 'translation' of NRCS to wind speed is not produced similarly to e.g. gridded ocean wind products from scatterometer. SAR data are provided in swath (and raw) mode only. Hence it is necessary to first calibrate the image; then apply a GMF algorithm for wind mapping. The advantage, however, is that the spatial resolution is much higher (compare ~1 km with ~25 km). The accuracy on wind speed and direction in SAR wind maps is similar to that of scatterometers.

ERS

ERS is the European Remote Sensing satellite from the European Space Agency (ESA). ERS-1 was launched in July 1991 and was operational to 2000. On-board was a C-band SAR with vertical receive, vertical transmit (VV) polarization. This imaging SAR provides maps of 100 km by 100 km with raw resolution ~25 m. In March 1995 ERS-2 with a similar SAR on-board was launched and this is still

operational. The wind maps obtained from ERS have a grid resolution of 400 m.

Envisat ASAR

ESA launched the Envisat satellite with an Advanced SAR on-board in March 2002. The ASAR is capable of recording in 37 different imaging SAR modes (one at a time). Some modes are similar to ERS; other modes are very different. The ASAR is a C-band SAR with VV, HH, VH and HV polarization capability. The VV polarization typically is preferred for wind retrieval as well established GMFs are available, e.g. (5, 11, 12). When estimating winds from HH, a polarization ratio between VV and HH is needed *a priori* (13, 14). The ASAR can record in swath up to 400 km wide. This is the so-called Wide Swath Mode (WSM). From Envisat WSM the resulting wind maps have grid cells ~1.6 km.

3. Offshore Wind Results

3.1 Long-term data series

Ocean wind from SSM/I is the source offering the longest time-series of observations. The observations are however somewhat far from the coastline as indicated in Figure 1.



Figure 1: SSM/I ocean wind map near Denmark.

The average wind speed during 10 years per month in the North Sea and the Baltic Sea is shown in Figure 2.

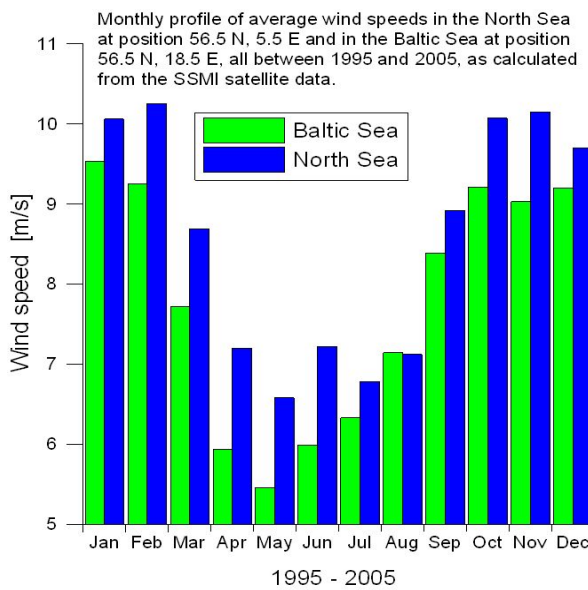


Figure 2: SSM/I ocean wind speed.

Ocean winds in the North Sea per year from SSM/I from 17 years is compared with winds from QuikSCAT and AMSR-E for five and two years, respectively, in Figure 3.

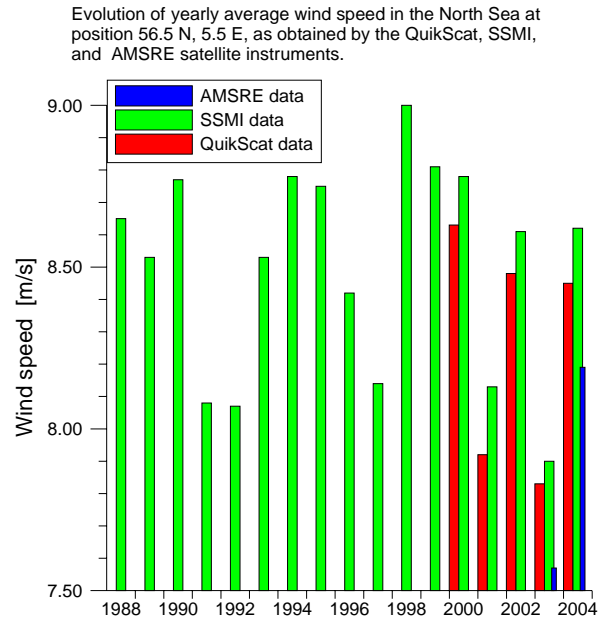


Figure 3: Annual ocean wind speed from SSM/I, QuikSCAT and AMSR-E.

3.1 Wind resource at low resolution

Ocean wind maps from QuikSCAT are provided in a 0.25° grid resolution as SSM/I winds. The near-coastal mask is much narrower in QuikSCAT than SSM/I. Figure 4 shows the mean winds for five years near Denmark observed from QuikSCAT.

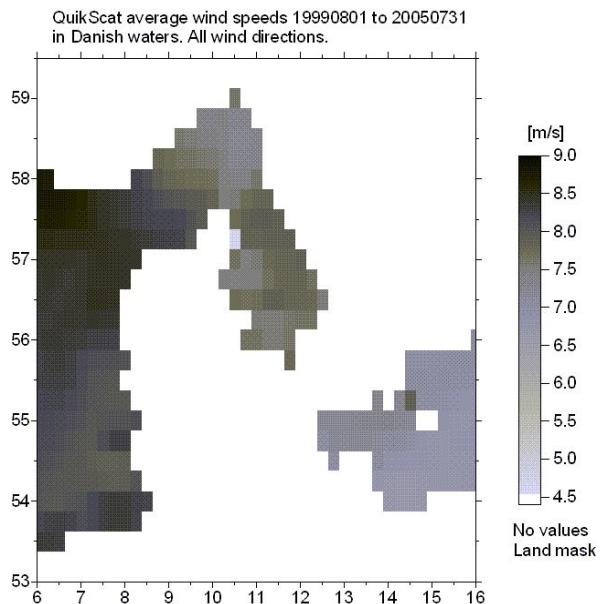


Figure 4: QuikSCAT ocean mean wind speed.

For wind resource estimation the Weibull A (scale) and k (shape) parameters are calculated. Resulting maps for the Danish waters are shown in Figure 5. The data are also available in WASP tab-file format.

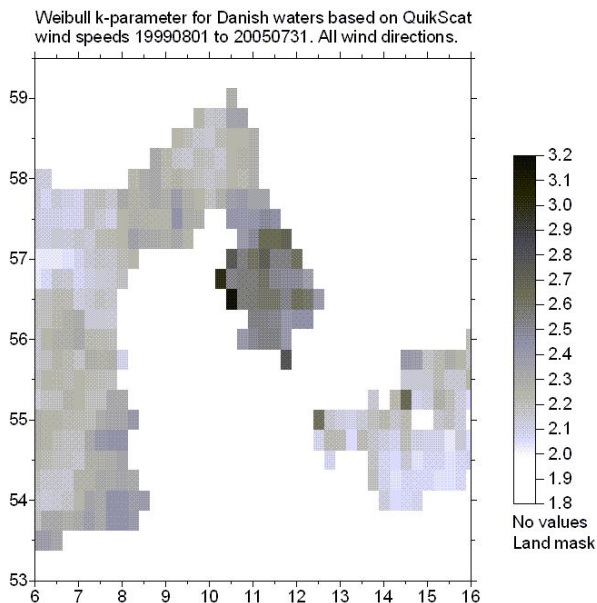
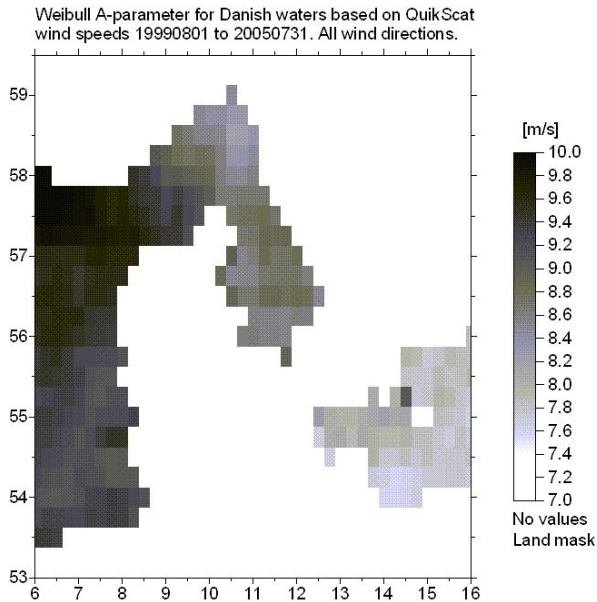


Figure 5. QuikSCAT wind statistics for five years for the Danish Seas. Upper panel: Weibull A; Lower: panel Weibull k parameter.

3.2 Wind resource at medium resolution

Envisat ASAR WSM wind maps are retrieved for the Danish Seas. A series of 25 maps have been calibrated and calculated into wind speed and wind direction using the Johns Hopkins University, Applied Physics Laboratory method and software. Wind direction is

estimated *a priori* with the NOGAPS meso-scale model and used as input to CMOD-4 (13, 15). The 25 maps are located as shown in figure 6.

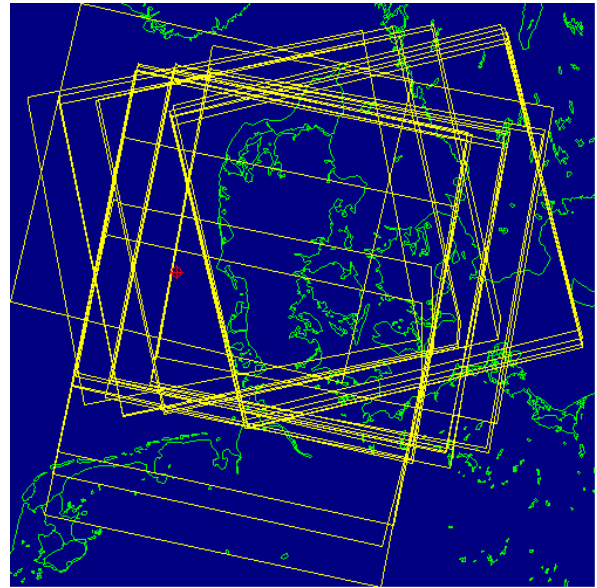


Figure 6. Location of 25 Envisat ASAR WSM wind maps retrieved for the Danish Seas.

In order to compare relative wind speed differences within a given domain, it is necessary to have full coverage of all images for the selected domain. From the above set of images only a small area in Southern Jutland is covered by all 25 wind maps. The resulting mean wind speed map is shown in figure 7. Excluding five wind maps allow a larger area to be covered as shown in figure 8. The wind rose corresponding to the 20 wind maps is shown in figure 9.

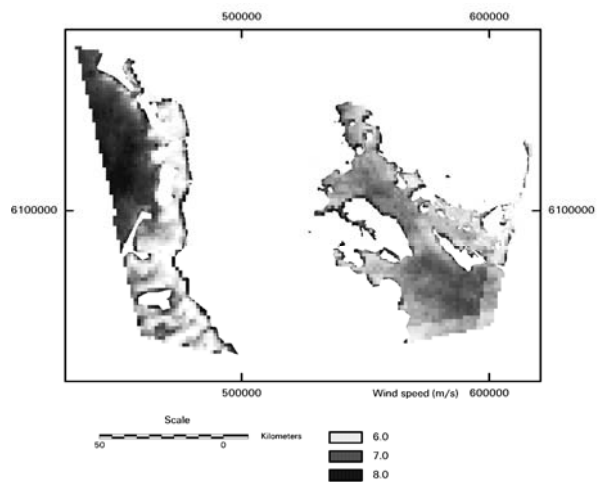


Figure 7. Mean wind speed offshore near Southern Jutland, Denmark from 25 Envisat ASAR WSM wind maps.

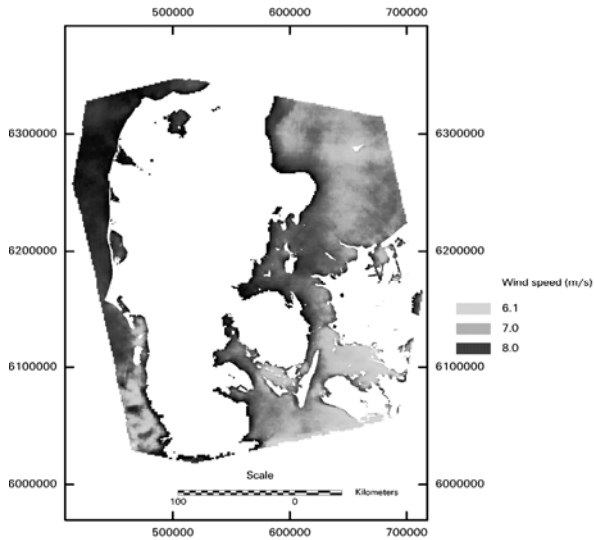


Figure 8. Mean wind speed offshore near Denmark from 20 Envisat ASAR WSM wind maps.

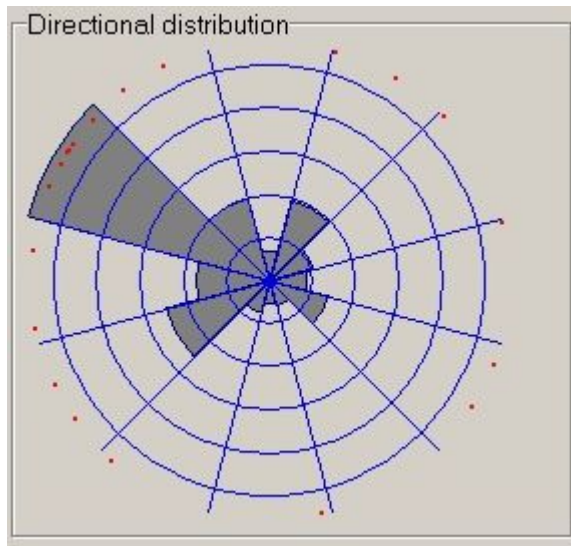


Figure 9. Wind rose from 20 Envisat ASAR WSM (near Horns Rev).

3.3 Wind resource at high resolution

Eighty-five ERS- 2 SAR wind maps are retrieved near Horns Rev in the North Sea. Figure 10 shows the location the 85 wind maps. Selecting a subset of 45 maps allows an area in the southern part of the North Sea to be mapped as shown in figure 11. Horizontal transect lines of mean wind speed, Weibull A and k values are graphed in figure 12. Wind speed retrieval in very shallow waters is not reliable. This is prevalent in the Wadden Sea and in figure 11 shaded pale gray. In figure 12 the false wind observations are indicated with 'Wind speed ?', 'Weibull A?', and Weibull k?'.

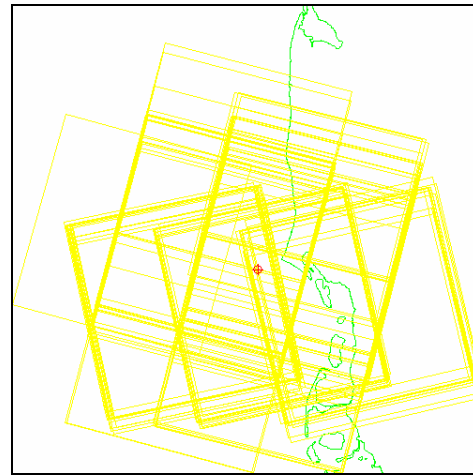


Figure10. Position of 85 ERS-2 SAR wind maps in the North Sea.

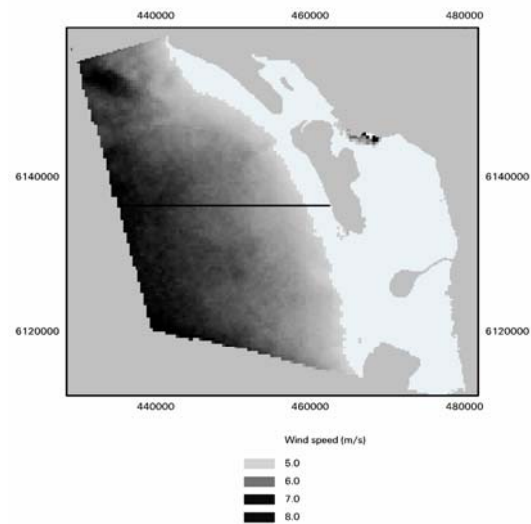


Figure11. Mean wind speed from 45 ERS-2 SAR wind maps in the southern part of the North Sea.

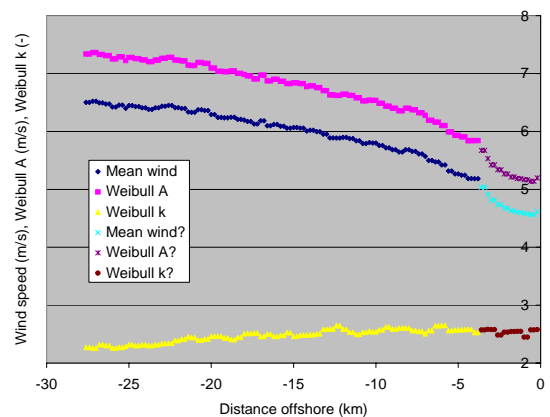


Figure 12. Mean wind speed along horizontal transect as located in figure 11 in the North Sea.

3.4 Wind farm wake effects

Two large offshore wind farms are located near Horns Rev and Nysted in the North Sea and Baltic Sea, respectively. In calm winds the turbines are clearly seen in wind speed maps from SAR as displayed in figure 13. Also shown is a case (1 March 2005) with windy conditions at Horns Rev.



Figure 13: Upper panel: Horns Rev wind farm in calm winds. Middle panel: Nysted wind farm in calm winds (from(16)). Lower panel: Horns Rev wind farm in windy conditions. Two parallel horizontal transect lines are shown, one through the wind farm the other in non-obstructed flow.

Observation of wind speed along the two horizontal

transect lines are shown in figure 14. Based on 12 SAR wind maps from ERS-2 and Envisat covering the wind farms at Horns Rev and Nysted, the average wake velocity deficit is calculated. The result is shown in figure 15. The velocity deficit (VD) is calculated from

$$VD = \frac{U_{freestream} - U_{wake}}{U_{freestream}} 100\%$$

where $U_{freestream}$ is observed in the non-obstructed horizontal transect and U_{wake} is observed upwind, within and downwind of the wind farm.

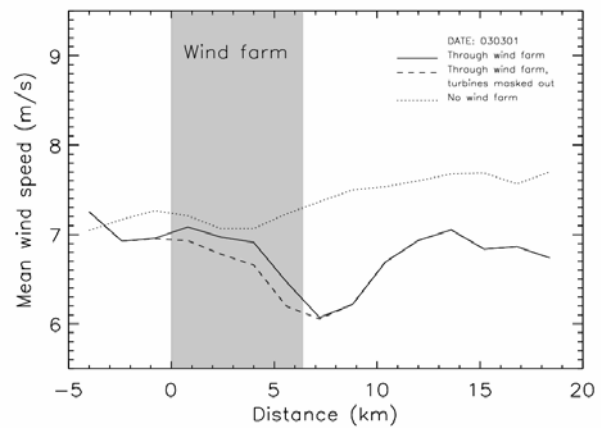


Figure 14: Wind speed observed through the Horns Rev wind farm and parallel to the wind farm from ERS-2 SAR.

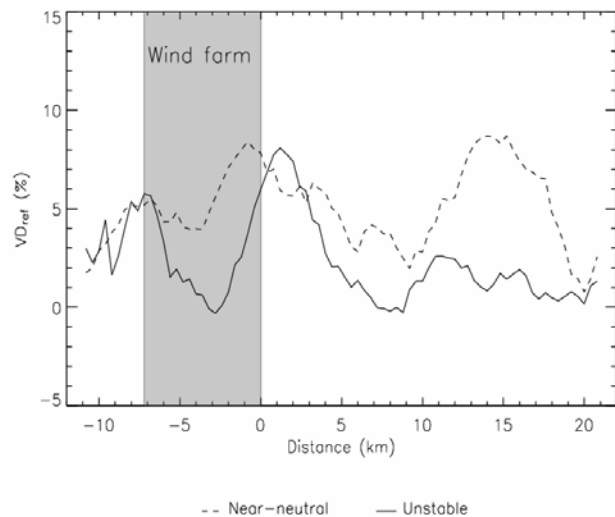


Figure 15: Wake velocity deficit mean values for nine near-neutral and three unstable cases observed from ERS-2 SAR and Envisat ASAR from Horn, from Horns Rev and Nysted combined (16).

3.5 Comparison of QuikSCAT and in-situ wind observations

At Horns Rev meteorological observations (wind speed at 15 m and wind direction at 28 above mean sea level) from a mast located 14 km offshore are compared to QuikSCAT winds. The result is shown in figure 16.

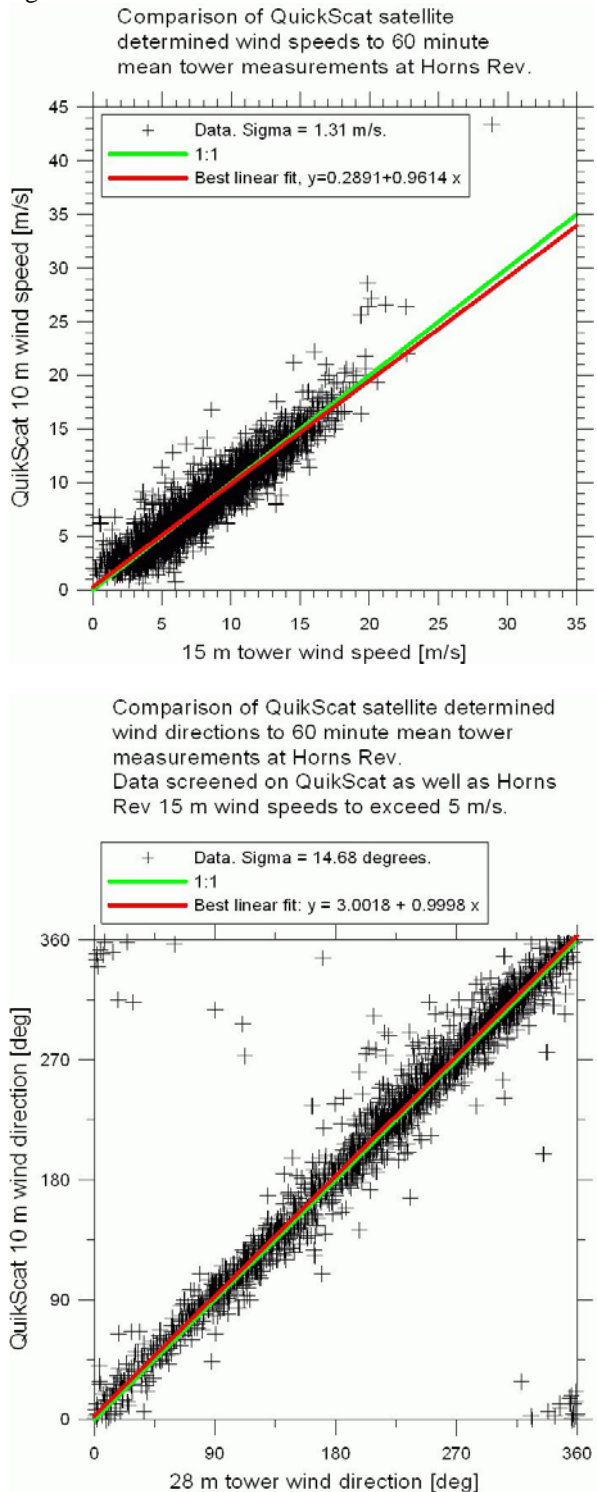


Figure 16: Comparison of wind speed at 15 m (upper panel) and wind direction at 28 m for $U > 5 \text{ ms}^{-1}$ (lower panel) from meteorological mast (tower) and QuikSCAT from 21 June 1999 to 31 December 2004.

Number of samples is are 3712 and 2359, respectively. Sigma is the standard deviation on QuikSCAT winds from the best fit linear regression lines.

4. Discussion

Ocean average wind speed in different spatial resolutions are calculated for the Danish Seas based on SSM/I, QuikSCAT, Envisat ASAR WSM and ERS-2 SAR observations. The most frequent observations are from SSM/I. Currently ocean winds are observed six times per day globally. Variations in the annual mean values for a grid cell in the North Sea is seen to vary by more than 1 ms^{-1} between a 'low wind year' (2003) and a 'high wind year' (1998) (fig. 3). This is based on 17 years of observations. SSM/I is the longest time-series on ocean winds. The information may be used for wind-indexing and for estimating wind climatology in general.

Monthly variations in average wind speed based on six daily observations for a decade for two locations are shown in fig. 2. It is seen that winds are higher in the North Sea than the Baltic Sea in all months except August. The lowest monthly mean winds are observed in May both in the Baltic Sea ($\sim 5.5 \text{ ms}^{-1}$) and in the North Sea ($\sim 6.5 \text{ ms}^{-1}$). The highest winds are observed in January in the Baltic Sea ($\sim 9.5 \text{ ms}^{-1}$) and in February in the North Sea ($\sim 10.2 \text{ ms}^{-1}$). SSM/I quantify ocean wind speed but not wind direction. The grid resolution is 0.25° but the coastal mask is $\sim 1^\circ$ wide thus the Danish Seas are not mapped.

QuikSCAT winds are mapped at a grid resolution of 0.25° similarly to SSM/I. Major differences are:

- 1) QuikSCAT has a narrower coastal mask than SSM/I.
- 2) QuikSCAT provides wind speed and direction (SSM/I wind speed only).
- 3) QuikSCAT observes twice per day (SSM/I observes six times).
- 4) QuikSCAT time-series contains 6 years of data (SSM/I contains 17 years of data).

Mean wind speed for 6 years in the Danish Seas mapped from QuikSCAT is shown in fig. 4. It is seen that ocean winds are higher in the northern part of the North Sea than in the southern part. Also winds in the Baltic Sea are lower than in the North Sea. The wind direction is also known. Therefore mean wind speed maps from four sectors (North, East, South and West) are calculated. These maps show the gradual speed up from the coast and offshore. With winds from North e.g. the lee effect of the Norwegian peninsula is very clear. The maps are not shown here. For wind resource estimation the Weibull A and k are used.

Ocean wind maps with these statistics are shown in fig. 5. The data are also available in WASP-tab-file format. It should be kept in mind that satellite-based winds are valid for 10 m above sea level. Therefore it is necessary to calculate the winds at hub-height using a model, e.g. the WASP program (17) as used for the European Wind Atlas (18).

QuikSCAT winds are observed some distance from the coastline, minimum 0.25° offshore. Offshore meteorological masts in wind farm projects typically are located closer to the coastline, e.g. at Horns Rev about 0.12° offshore. It has been chosen, however, to compare the observed winds at the Horns Rev mast with the nearest grid cell in the QuikSCAT maps during the period 21 June 1999 to 31 December 2004. The number of samples is 3712. The result is shown in fig. 16 and the overall fit is very promising. Annual mean values of QuikSCAT observations in a grid cell in the North Sea covered both by SSM/I, QuikSCAT and AMSR-E are compared in fig. 3. From this it is seen that QuikSCAT observe winds slightly lower than the SSM/I observations. The data from AMSR-E are much lower for the two years available.

Even though QuikSCAT has a coastal mask that is narrower than the one for SSM/I ocean winds, QuikSCAT does not directly map ocean winds for the coastal zone relevant for wind engineering. Wind farm activities typically take place within a 30 km zone from the coastline. It may be possible to use the QuikSCAT winds through modeling activity to provide estimates for the coastal zone. Another option is to use satellite imaging SAR wind observations. These observations are right on the spot of interest.

Ocean winds observed from Envisat ASAR WSM are accessible since March 2002. In the first year of operation a limited number of this type of SAR images were collected. This was due to several other modes (37 modes can be chosen) of observations being collected. In late 2003 it was found that most satellite image users would prefer the WSM (VV) mode of observation, and therefore the ESA archive contains many images (<http://eoli.esa.int/>) of this type since then. The major advantage of WSM is that it covers 400 km by 400 km in one snapshot with a grid resolution in e.g. wind maps of ~ 1.6 km. Envisat WSM wind maps are compared to atmospheric model results for a few cases in the Baltic and North Sea (9).

The mean wind speed of 20 maps for the Danish Seas is shown in fig. 8 and a smaller area based on 25 wind maps in fig. 7. The results are preliminary and comparison to other observations and models are in progress. Some of the research topics are to study the wind statistics per sector and describe the variations in wind speed as a function of wind direction and

distance to shoreline. The maps allow to link between the coastline and the QuikSCAT observations.

Prior to the Envisat ASAR WSM observations, the high-resolution C-band SAR with VV from ERS-1 and ERS-2 has constituted a very significant contribution to ocean wind mapping. These observations allow small spatial details to be mapped. Earlier studies on the accuracy of wind from ERS-2 SAR are reported (19). The results are similar to the QuikSCAT results in fig. 16. It is important to select the high-resolution wind maps carefully so that a sufficiently large area is mapped in all wind maps. Fig. 11 shows an example near Horns Rev and the variation in mean wind speed, Weibull A and k along a horizontal transect line is shown in fig. 12. In a zone of ~ 5 km from the island Rømø the wind observations are disturbed by the coastal activity (combination of sea bottom, waves, currents and atmospheric effects).

As demonstrated in the studies by (20, 21) it is necessary to select a sufficient number of samples (images) if e.g. 10% accuracy at 90% confidence level is required. For mean wind speed the number of samples needed is ~ 70 , yet for Weibull A and k considerably higher numbers. In addition the accuracy of satellite observations listed earlier in this paper should be added to the uncertainty. The studies of (20, 21) assumes all samples to be perfectly accurate and to be distributed randomly in time. Satellite images are sampled regularly in time as they all fly in orbits with local crossing times at selected hours. For sites with significant diurnal variation this adds to the overall uncertainty in satellite-based wind resource estimates.

Wind resource statistics based on SAR wind maps are obtained from the Risø Wemsar Tool (RWT) software developed first in the EU-WEMSAR project and more recently upgraded in the EO-windfarm project. Details on RWT are available in (22, 23). The Wemsartool for ERS SAR image wind retrieval is described in (24). The wake analysis results provide a spatial mapping of the length, the width and the intensity of wake velocity deficit (16, 25). The results are the first of their kind.

5. Conclusion

Wind mapping offshore based on satellite images contributes a complementary source of information on the offshore wind resources in the Danish Seas. Comparison results to meteorological mast observations are encouraging for applied use in pre-feasibility wind mapping. Offshore wind resource model results will be compared to the wind climatology observed from satellite observations at various spatial scales in the near future.

Acknowledgements

Funding from the Danish Research Agency STVE Sagsnr. 2058-03-0006 (SAT-WIND), STVF Sagsnr. 26-02-0312 (SAR-WAKE) and from ESA EOMD 17736/03/I-IW (EO-windfarm) is greatly appreciated. Satellite data from ESA (Cat. 1 EO-1356) project is acknowledged. We are thankful to all institutes that allow free access to satellite-based ocean wind maps based on QuikSCAT, AMSR-E and SSM/I. Our cooperation with F. Monaldo and D. Thompson at Johns Hopkins University, Applied Physics Lab., Maryland, USA for hosting Ph.D. student Merete B. Christiansen is greatly appreciated as well as access to the JHU/APL near-real-time software. Meteorological data are kindly provided by Elsam Engineering.

References

1. Executive Committee for IEA. "IEA Wind Energy. Annual Report 2004." 2005.
2. European Wind Energy Association. "Imagine energy without fuel, EWEA." No. http://www.ewea.org/documents/051021_WD_OilSupply.pdf, 2005.
3. H.J.Kramer. *Observation on the Earth and Its Environment. Survey of missions and sensors*, Berlin: Springer, 2002.
4. F.J.Wentz. "A well calibrated ocean algorithm for SSM/I." No. 101395, *Remote Sensing Systems*, Santa Rosa, CA, 1995.
5. A.Stoffelen and D.L.T.Anderson. "Scatterometer data interpretation: Estimation and validation of the transfer function CMOD4." *Journal of Geophysical Research* 102, no. C3(1997):5767-80.
6. T.W.Gerling. "Structure of the surface wind field from the SEASAT SAR." *Journal of Geophysical Research* 91, no. C2(1986):2308-20.
7. S.Lehner, J.Horstmann, W.Koch, and W.Rosenthal. "Mesoscale wind measurements using recalibrated ERS SAR images." *Journal of Geophysical Research* 103, no. C4(1998):7847-56.
8. Y.Du, P.W.Vachon, and J.Wolfe. "Wind direction estimation from SAR images of the ocean using wavelet analysis." *Canadian Journal of Remote Sensing* 28, no. 3(2002):498-509.
9. J.Horstmann, W.Koch, and S.Lehner. "Ocean wind fields retrieved from the advanced synthetic aperture radar aboard ENVISAT." *Ocean Dynamics* 54, no. 6(2004):570-76.
10. W.Koch. "Directional analysis of SAR images aiming at wind direction." *IEEE Transactions on Geoscience and Remote Sensing* 42, no. 4(2004):702-10.
11. J.Figa-Saldana, J.J.W.Wilson, E.Attema, R.Gelsthorpe, M.R.Drinkwater, and A.Stoffelen. "The advanced scatterometer (ASCAT) on the meteorological operational (MetOp) platform: A follow on for European wind scatterometers." *Canadian Journal of Remote Sensing* 28, no. 3(2002):404-12.
12. Y.Quilfen, B.Chapron, T.Elfohaily, K.Katsaros, J.Tournadre, and B.Chapron. "Observation of tropical cyclones by high-resolution scatterometry." *Journal of Geophysical Research* 103, no. C4(1998):7767-86.
13. F.Monaldo, D.R.Thompson, W.Pichel, and P.Clemente-Colón. "A systematic comparison of QuickSCAT and SAR ocean surface wind speeds." *IEEE* 42, no. 2(2004):283-91.
14. A.A.Mouche, D.Hauser, J.F.Daloz, and C.Guerin. "Dual-polarization measurements at C-band over the ocean: Results from airborne radar observations and comparison with ENVISAT ASAR data." *IEEE Transactions on Geoscience and Remote Sensing* 43, no. 4(2005):753-69.
15. F.Monaldo, V.Kerbaol, P.Clemente-Colón, B.Furevik, J.Horstmann, J.Johannessen, X.Li, W.Pichel, T.D.Sikora, D.J.Thomson, and C.Wackerman. "The SAR measurement of ocean surface winds:an overview." pp. 15-32. *Proceedings of the Second Workshop Coastal and Marine Applications of SAR*, 2-12 September 2003, Svalbard, Norway, ESA, 2003.
16. M.B.Christiansen and C.B.Hasager. "Wake effects of large offshore wind farms identified from satellite SAR." *Remote Sensing of Environment* 98,(2005):251-68.
17. N.G.MORTENSEN, D.N.Heathfield, L.Landberg, O.Rathmann, I.TROEN, and E.L.Petersen. "Wind Atlas Analysis and Wind Atlas Analysis and Application program:WAsP 7.0 Help Facility." No. ISBN 87-550-2667-2, Risø National Laboratory, Roskilde, 2000.
18. I.Troen and E.L.Petersen. *European Wind Atlas*, Roskilde: Risø National Laboratory, 1989.
19. C.B.Hasager, E.Dellwik, M.Nielsen, and B.Furevik. "Validation of ERS-2 SAR offshore wind-speed maps in the North Sea." *International Journal of Remote Sensing* 25, no. 19(2004):3817-41.
20. S.C.Pryor, M.Nielsen, R.J.Barthelmie, and J.Mann. "Can satellite sampling of offshore wind speeds realistically represent wind speed distributions? Part II Quantifying uncertainties associated with sampling strategy and distribution fitting methods." *Journal of Applied Meteorology* 43,(2004):739-50.
21. R.J.Barthelmie and S.C.Pryor. "Can satellite sampling of offshore wind speeds realistically represent wind speed distributions." *Journal of Applied Meteorology* 42, no. 1(2003):83-94.
22. M.Nielsen, P.Astrup, C.B.Hasager, R.J.Barthelmie, and S.C.Pryor. "Satellite information for wind energy applications." No. Risø-R-1479(EN), Risø National Laboratory, Roskilde, Denmark, 2004.
23. C.B.Hasager, M.Nielsen, and M.B.Christiansen. "RWT tool: offshore wind energy mapping from SAR." SP-572 *Envisat/ERS Symposium Proceedings*, 6-10 September 2004, Salzburg, Austria, 2004.
24. B.Furevik and H.Espedal. "Wind Energy Mapping using SAR, *Canadian Journal of Remote Sensing*, Special issue: Woman Sensing the World (WSW)." *Can. J. Remote Sensing* 28, no. 2(2002):196-20
25. M.B.Christiansen and C.B.Hasager. "Using airborne and satellite SAR for wake mapping offshore." 2005.